*Applied Numerical Modeling in Geomechanics – 2020 – Billaux, Hazzard, Nelson & Schöpfer (eds.) Paper: 11-09*


# Simulation of paste backfill material with *FLAC3D* at Kittilä

Amélie Ouellet[1], Thierry Lavoie[1], Antti Pyy[2], Louis-Philippe Gélinas[3], Véronique Falmagne[3] & Patrick Andrieux[1]

[1] *Andrieux & Associates Geomechanics Consulting, Montreal, Canada*

[2] *Agnico Eagle Mines, Kittilä Mine, Kittilä, Finland*

[3] *Agnico Eagle Mines, Technical Services, Preissac, Canada*

## 1 INTRODUCTION

A malfunction at the paste backfill plant at the Agnico Eagle Kittilä gold mine in Lapland in northern Finland resulted in several primary stopes towards the center of production pyramids being filled with sub-standard paste fill material, which exhibited weak ultimate strength and low stiffness. The ultimate (over 25 days) unconfined compressive strength (UCS) values obtained in the laboratory were low – mostly below 500 kPa – and highly scattered with coefficients of variation over 20% and up to 50%. Moreover, UCS tests on in situ samples resulted in significantly weaker values than tests conducted on plant samples. As an example, the average UCS of 10 plant tests conducted for one stope was 410 kPa, while the average of the 3 corresponding in situ tests was as low as 25 kPa. Furthermore, visual observations of paste core showed in some instances very soft – almost plasticine-like – conditions.

This, in turn, raised questions on the behavior of that material once exposed by future secondary mining further along the sequence. *FLAC3D* (Itasca 2017) is well adapted to the simulation of paste backfill material in underground mining and is routinely used to examine its mechanical behavior when laterally exposed by secondary or tertiary mining or undercut. Consequently, numerical *FLAC3D* analyses were conducted to simulate the performance of this poor-quality backfill and investigate potential mining scenarios to recover abutting secondary stopes while minimizing dilution from that material.

A back-analysis was first conducted to better understand the poor-quality paste strength properties. The calibration case consisted of a secondary stope that had been blasted next to poor-quality paste. Strength properties were adjusted to best reproduce the available cavity monitoring survey (CMS) scans, which indicated paste dilution into that secondary stope. From this calibration exercise, it was found that the implemented strength of the paste backfill should vary along the stope height, with stronger paste being found at the bottom of the stope and weaker paste being found at the top. It was also found that paste should initially be placed in the model as a fluid, which subsequently solidifies into a solid material. This paper focuses on those two modelling approaches, which were then used in forward analyses to evaluate recovery options for stopes abutting poor-quality paste.

## 2 BACK-ANALYSIS METHODOLOGY

The back-analysis consisted of a case where a secondary stope has been excavated next to poor-quality paste. Two CMS scans indicating paste dilution into the secondary stope were available: one less than halfway through mucking operations and the other at the end of mucking.

A small-scale model subjected to gravity alone was built to reproduce this situation. Two stopes were included in the model: one primary stope filled with poor-quality paste, and one abutting secondary stope to

be excavated. The dimensions of the stopes were 16 m (N-S: longitudinal) by 18 m (E-W: transverse) by 40 m (vertical height) with a dip of 75 degrees. The surrounding rock mass was modelled as an elastic material. The paste material was modelled as a strain-softening Mohr-Coulomb material. However, the weakest paste material (with a UCS value under 85 kPa, based upon the results of the calibration exercise, and supported by Fall 2007 observations) was modelled as a perfectly plastic medium (with the residual cohesion and friction equal to their peak values). This model was only gravity-loaded because it focused on the paste behavior, and because the density and stiffness contrast between the paste and the surrounding rock mass was high (a density of about 1.2 for the paste, and around 2.7 for the rock mass; a Young's modulus of approximately 200 MPa for the paste, and 1 GPa for the rock mass) – these contrasts allowed for the stress distribution within the paste to be analyzed separately from that of the rock mass.

The poor-quality paste strength properties were adjusted to best reproduce the failure shape shown by the CMS scans conducted during the mining of the neighboring secondary stope. The model indicators used to conclude on the fitting of the failure shape were velocity and yielding/plasticity. Gridpoints with velocities greater than 1e-5 at equilibrium were considered to be in failure. Note that the gridpoint velocity is not the actual physical velocity since various numerical scaling procedures are being applied to speed the model to convergence. The velocities in this study are being used in a relative sense to delineate the volumes of failure.

Calibration was reached by adjusting the paste's UCS values and strength gradation. Tension was linked to the cohesion value. A ratio of 12% (tension/cohesion) was found to give good calibration results. The models were considered to be at equilibrium when the mechanical ratio reached the value of 1e-5. In some cases, when the poor-quality paste was in failure, the model did not reach equilibrium and cycling was stopped at a point where the failure shape seemed, based on gridpoint velocity, to have stabilized. The number of cycles for each modelling step is shown in the figures provided, as well as information about the equilibrium state (at equilibrium vs still unstable).

## 3 MODELLING RULES FOR PAST BACKFILL IMPLEMENTATION

### 3.1 *Effect of past strength variation with stope height*

Available UCS tests (both plant and in situ) were used to guide the calibration process. The UCS values that best matched the laboratory results and the CMS data showed a significant strength variation along the paste column height, with strength higher at the bottom of the column and lower at the top. The UCS values eventually retained after the calibration exercise varied between 285 kPa at the bottom and as low as 15 kPa at the top of the column, changing linearly along the column height in 15 kPa increments every 2 m.

The calibrated 285 kPa UCS value at the bottom of the stope corresponded to the $10^{th}$ percentile of the plant test results, whereas the 15 kPa UCS at the top of the stope was close to the weakest in situ test result (11 kPa). Modelling results with the calibrated properties are shown in Figures 1 & 2. Gridpoints with a velocity greater than 1e-5 at equilibrium (in red in the figures) closely matched both CMS shapes (Fig. 1), with a shear failure band generally following the CMS shapes, and the poor-quality paste remaining largely intact below that shear band. Tensile failure suggesting raveling was observed above the shear band.

To demonstrate the necessity to implement a variable strength in the paste, modelling results in which a unique strength value was assigned to paste are shown in Figure 3. In that model, a UCS value of 142 kPa was uniformly assigned to the paste. Based on the velocity plots, and assuming gridpoints with a velocity greater than 1e-5 at equilibrium are in failure, the final failure shape was wider than the actual CMS-derived shape (Fig. 3b). If a stronger UCS value was implemented, no failure at all was predicted in the paste. Furthermore, no failure was predicted after partial mucking, which was not in agreement with the first CMS scan (Fig. 3a). If a weaker UCS value was implemented to predict failure at that step, the final failure shape grew even wider, which then now did not match the second CMS scan.

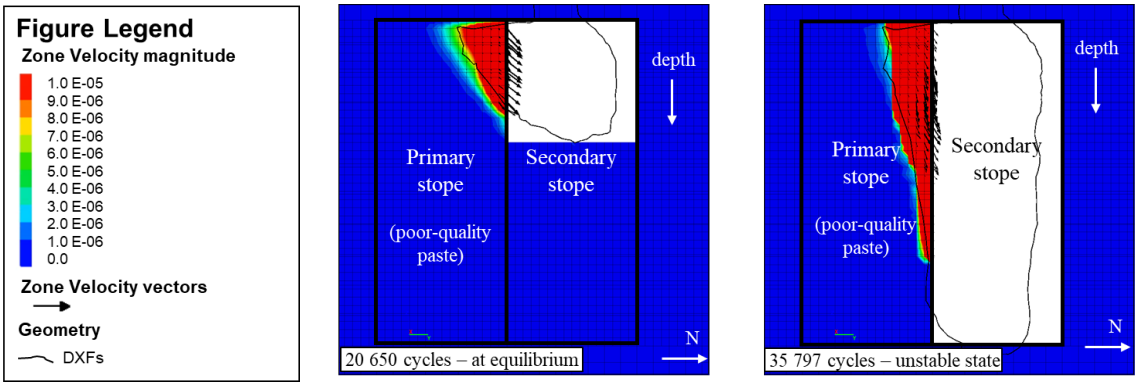


(a) Partial mucking. (b) Complete mucking.

Figure 1. Velocity plots for the calibration case. UCS at the bottom of the stope: 285 kPa; UCS at the top of the stope: 15 kPa. Cross-sections cut half-way between the hanging wall and footwall, with solid rock all around.

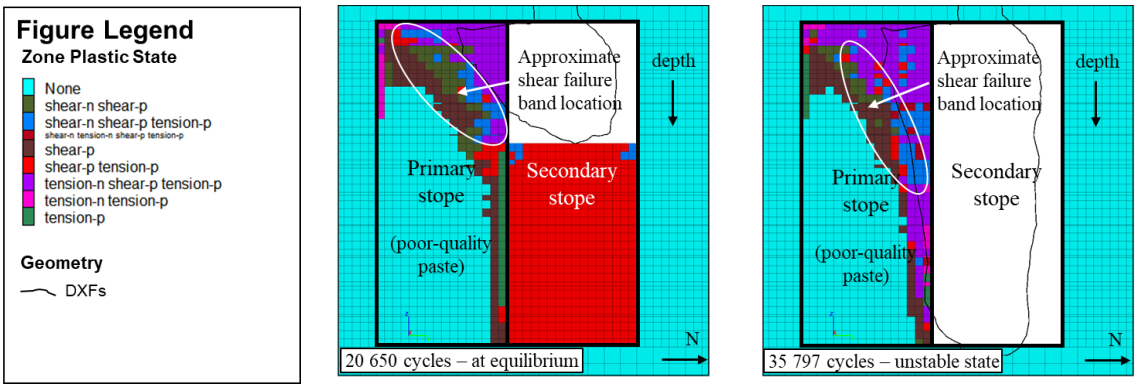


(a) After partial mucking. (b) After complete mucking.

Figure 2. Plastic state plots for the calibration case. UCS at the bottom of the stope: 285 kPa; UCS at the top of the stope: 15 kPa. Cross-sections cut half-way between the hanging wall and footwall, with solid rock all around.

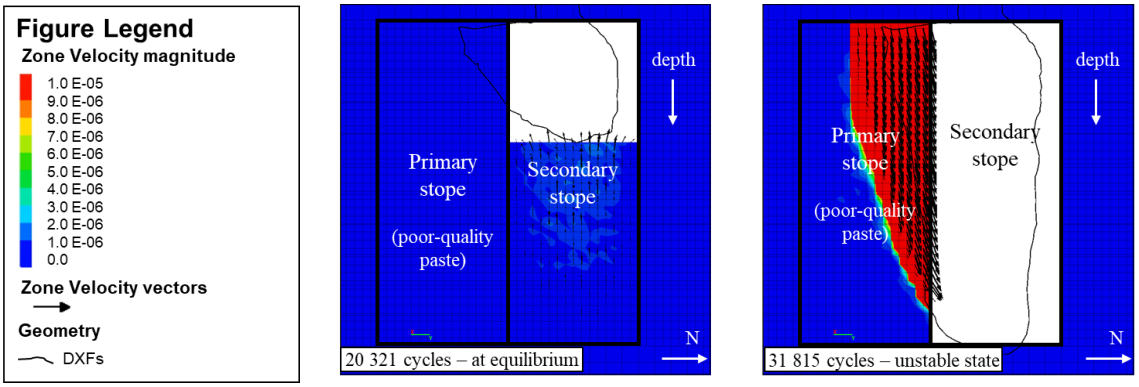


(a) Partial mucking. (b) Complete mucking.

Figure 3. Velocity plots for the calibration case with a uniform paste strength of 142 kPa. Cross-sections cut half-way between the hanging wall and footwall, with solid rock all around.

### 3.2 *Effect of liquid-to-solid paste placement initialization*

Once initial pre-mining equilibrium has been reached, the typical steps to place paste backfill in a stope consist of extracting the stope, cycling to equilibrium, placing (solid) paste material and cycling to equilibrium for loads to develop throughout the paste volume.

However, this sequence of events fails to recognize that paste fill is initially placed as a fluid, which subsequently solidifies into a solid material. This affects the initial stress distribution throughout the fill material. Because the poor-quality paste strength appears to be very low (UCS values smaller than 500 kPa in most plant and in situ tests), it was expected that the paste behavior would be very sensitive to the stress distribution. Therefore, to best reproduce the stress distribution in the paste, it was in this case first considered as a viscous fluid (cohesionless and tensionless, with only friction), cycled to equilibrium in that state, and only then turned into a solid (with the calibrated mechanical properties) and equilibrated again to allow loads to develop throughout the paste volume.

A comparison between stress distributions in the poor-quality paste with a two-step (liquid-to-solid) and a one-step (directly solid) paste placement initialization is shown in Figures 4 & 5. When installing paste backfill in a single "solid" step, the equilibrated stresses tend to be more uniform throughout the volume and overall lower, particularly towards the bottom of the column (Fig. 4a). On the other hand, paste installed in two steps ends up exhibiting a more banded stress distribution along the *z*-axis (depth), more akin to that in a fluid, and overall higher internal loads (Fig. 4b). The confinement profile also shows significant differences, with the core confinement corridor being narrower in the one-step installation (Fig. 5). It should be noted that the models shown in Figures 4 & 5 have reached equilibrium (mechanical ratio of 1e-5) at a similar number of cycles. It was confirmed that the number of modelling cycles was sufficient, and that additional cycling did not change the stress distribution.

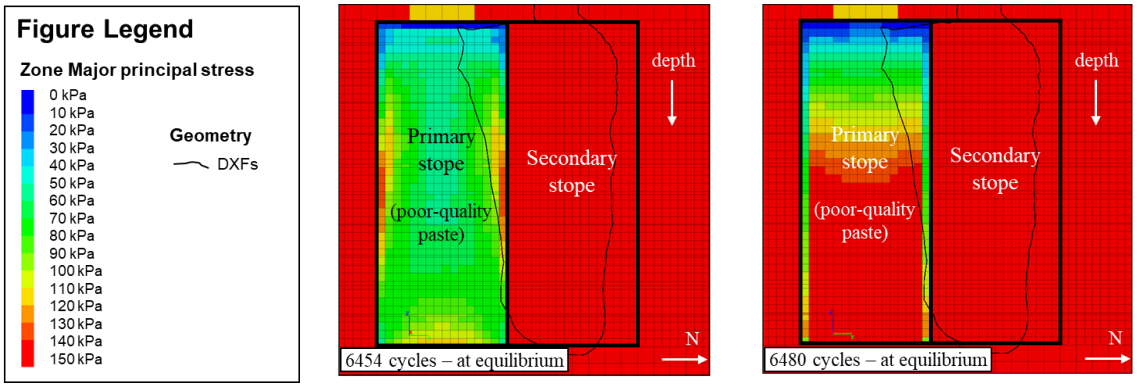


(a) Directly installed as a solid. (b) Installed first as a fluid, then as a solid.

Figure 4. Plots of $\sigma_1$ major principal stress magnitude in the paste material. UCS at the bottom of the stope: 285 kPa; UCS at the top of the stope: 15 kPa. Cross-sections cut half-way between the hanging wall and footwall, with solid rock all around.

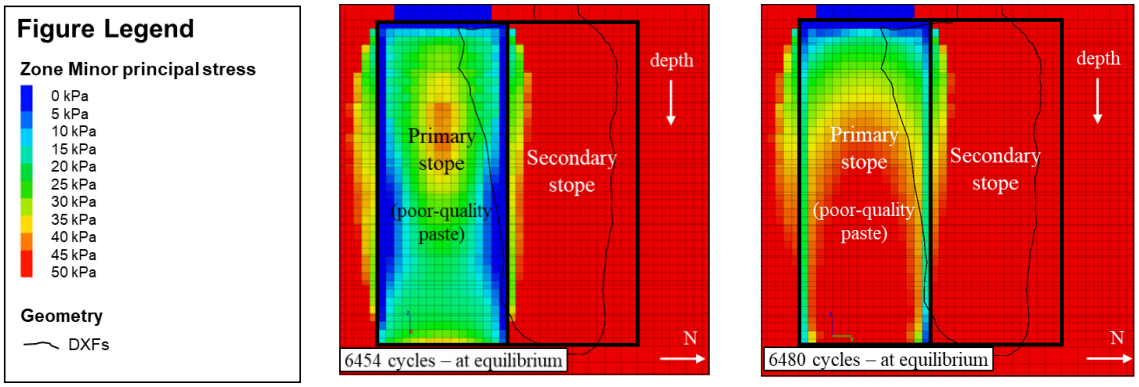


(a) Directly installed as a solid. (b) Installed first as a fluid, then as a solid.

Figure 5. Plots of $\sigma_3$ minor principal stress magnitude in the paste material. UCS at the bottom of the stope: 285 kPa; UCS at the top of the stope: 15 kPa. Cross-sections cut half-way between the hanging wall and footwall, with solid rock all around.

These initial load distribution differences lead to different mechanical behaviors once the paste is exposed. Results where paste was placed in one step (directly as a solid) are shown in Figure 6: note the lower fitting with the CMS scan compared to the two-step paste placement initialization shown in Figure 1.

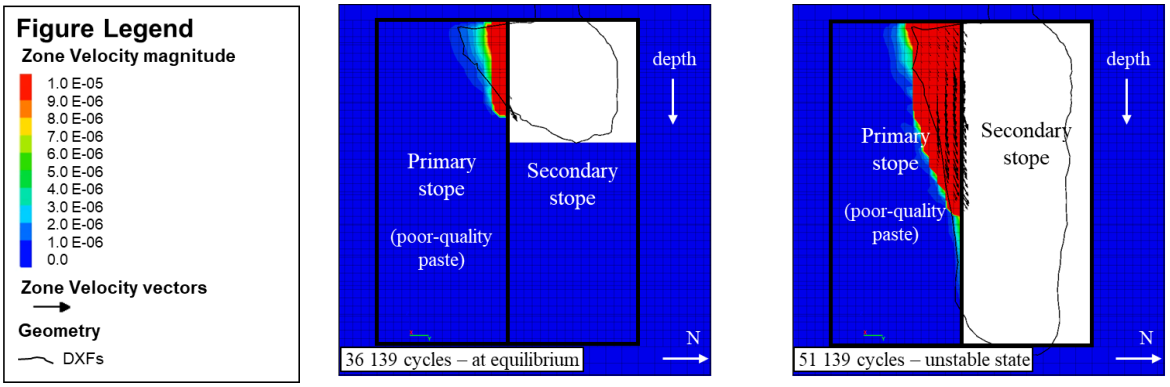


(a) Partial mucking. (b) Complete mucking.

Figure 6. Velocity plots for the calibration case with a one-step (directly solid) paste placement initialization. UCS at the bottom of the stope: 285 kPa; UCS at the top of the stope: 15 kPa. Cross-sections cut half-way between the hanging wall and footwall, with solid rock all around.

## 4 FORWARD ANALYSES

Following the calibration exercise, several mining scenarios were evaluated to recover secondary stopes abutting poor-quality paste material. One option evaluated consisted in removing the poor-quality paste, replacing it by stronger paste material and resuming mining. The feasibility of removing the paste was tested by simulating in *FLAC3D* various undercut geometries and evaluating whether the paste would fail based on velocity and yielding/plasticity indicators. If the paste volume was found to be in failure, it was assumed that it could be mucked and then replaced by stronger paste. Despite the low strengths considered, none of the undercut geometries simulated resulted in the complete collapse of the paste – this was largely due to some arching developing in the roof of the paste material, thus stabilizing it. Initial undercutting field tests confirmed that assessment.

The option of mining next to the poor-quality paste was then assessed, either with or without leaving a rock pillar against it. Various rock pillar thicknesses and shapes were evaluated to maximize ore recovery. Alternatively, the maximum height of poor-quality paste material expected to remain stable when exposed was evaluated. The main risks associated with these options were the failure of the pillar and/or the instability of the exposed weak paste.

## 5 CONCLUSIONS

Two modelling approaches for simulating paste backfill behavior were discussed in this paper. First, it was demonstrated that installing paste backfill in a two-step process – first as a fluid, then a solid – results in different internal loads developing throughout the paste volume, which, in turn, results in different behaviors. Second, it was shown that in cases where strength is not constant over the height of the column, the difference also needs to be accounted for in the model, which can be done based on laboratory tests combined with CMS measurements.

## REFERENCES

Itasca Consulting Group, Inc. 2017. *FLAC3D – Fast Lagrangian Analysis of Continua in 3 Dimensions, Ver. 7.0 User's Manual*. Itasca: Minneapolis.

Fall, M., Belem, T., Samb, S. & Benzaazoua, M. 2007. Experimental characterization of the stress–strain behaviour of cemented paste backfill in compression. Journal of Materials Science, vol. 42, pp. 3914–3922.